ORIGINAL ARTICLE

Catarina Pereira · Fernando Caldeira Jorge · Mark Irle
José Maria Ferreira

Characterizing the setting of cement when mixed with cork, blue gum, or maritime pine, grown in Portugal II: X-ray diffraction and differential thermal analyzes

Abstract It is already known by the scientific and industrial communities that lignocellulosic substrates are, to a certain extent, inhibitors of the hydration reaction of cement. The extent to which and how they influence such reactions is still a matter of debate. Several techniques, such as calorimetry, i.e., the measurement of the heat evolved or obtaining temperature profiles during the hydration, the determination of extractive contents of lignocellulosic substrates and their relation with the characteristics of the hydration curves, or even testing of the mechanical properties of the wood–cement composites, have been used in previous research. This study complements past research using two techniques that have been used in the analysis of cement hydration but are not usually applied to lignocellulose–cement mixes, namely X-ray diffraction (XRD) and differential thermal analysis (DTA). The raw materials for this study were three lignocellulosic materials of Portuguese origin: cork (the bark of *Quercus suber* L.), blue gum (*Eucalyptus globulus* Labill.), and maritime pine (*Pinus pinaster* Ait); and Portland cement. The two techniques allowed tracking of the evolution of the main cement constituents during hydration. It was found that all the lignocellulosic substrates had detrimental effects on cement hydration. The blue gum exhibited the fastest hydration kinetics in the initial stage of reaction, but was then overtaken by cork, which at the end gave the highest hydration conversion amongst the three lignocellulosic substrates. Although pine caused the slowest initial hydration kinetics, with the passage of time its effect approached that of blue gum. At the end of the hydration period, specimens containing either species had similar quantities of hydration reaction products. The DTA and XRD results were consistent and are in good agreement with the temperature profiles and compatibility indexes reported in a previous work.

Key words Cement · Wood · Cork · X-ray diffraction · Differential thermal analysis

Introduction

Cement-bonded wood composites have some advantages over many common wood composites in which the binder is a synthetic resin. Wood–cement composites exhibit better dimensional stability[1] and higher resistance to deterioration by fungi and insects, and to fire than other synthetic-binder composites.[2–5] Cement binder does not contain formaldehyde, which means formaldehyde emissions from these products are negligible. In addition, wood–cement composites have a greater resistance to adverse climatic conditions than wood,[2,3] although are not as good as concrete. These composites can be made with wood residues,[6] including recycled wood treated with preservatives,[7] and these residues can cause problems when used in combination with common synthetic resins. The main application for wood–cement panels is civil construction, including low-cost housing for developing countries,[8] but such composites can also be made in the form of lightweight, low-cost concrete blocks.[9]

Despite all these advantages, lignocellulosic materials of many different kinds, when combined with cement for composites, may not result in materials with satisfactory properties. In fact, mixing lignocellulosic material with cement paste usually interferes in the cement hydration reactions and might degrade the final properties of the composites. This negative effect on hydration is usually known as incompatibility, the outcome of which might be delayed setting time and reduced mechanical performance of the composite. Although until some time ago, it was impossible
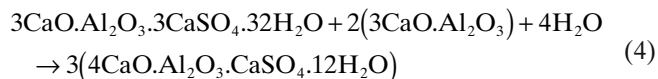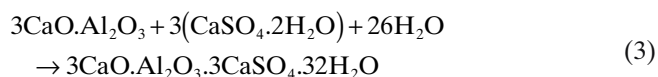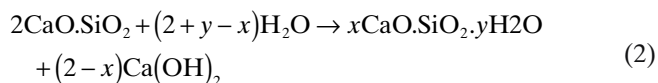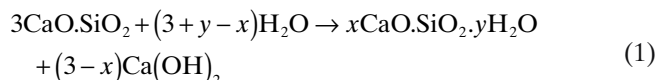
C. Pereira · J.M. Ferreira
Department of Ceramics and Glass Engineering – CICECO, University of Aveiro, Aveiro 3810-193, Portugal

F.C. Jorge (✉)
CEMAS – Centre of Modelling Studies and Environmental Systems Analysis Fernando Pessoa University, Praça 9 de Abril, 349 Porto 4249-004, Portugal
Tel. +351-91-909-2704; Fax +351-225-508-269
e-mail: fjorge@mail.ufp.pt

M. Irle
Ecole Supérieure du Bois, B.P. 10605, Rue Christian Pauc, Nantes 44306, Cedex 3, France

to identify the specific substance(s) in the lignocellulosic material that cause these negative effects, it was known that sugars and other extractives play a fundamental role.[10,11] Miller and Moslemi[3] found that some substances such as cellulose, lignin fatty acids, resin acids, sterols, and terpenes, at concentrations lower than 1.0%, did not cause significant negative effects on the tensile strength of wood–cement composites. However, they also found that glucose caused the greatest reduction in tensile strength, while substances such as hemicelluloses, tannins, and acetic acid caused some reduction.[3] What is somewhat contradictory in their work is that they found hemicelluloses and tannins to have the most detrimental effect on the hydration temperature profiles, especially on the maximum temperature attained and time to reach maximum temperature.[3]

Portland cement is a hydraulic binder that sets and hardens by chemical interaction with water and is capable of doing so under water.[12] The principal constituents of Portland cement are: tricalcium silicate ($3CaO.SiO_2$, represented by C_3S); dicalcium silicate in the beta modification ($2CaO.SiO_2$, βC_2S); tricalcium aluminate ($3CaO.Al_2O_3$, C_3A); tetracalcium aluminoferrite ($4CaO.Al_2O_3.Fe_2O_3$, C_4AF); and calcium sulfate dihydrate ($CaSO_4.2H_2O$, $C\bar{S}H_2$) added to cement clinker. The reaction between the main constituents of Portland cement and water can be summarized, very simply, by Eqs. 1–4.[13] They do not, however, convey the real complexity of the reactions that occur:

$$3CaO.SiO_2 + (3+y-x)H_2O \rightarrow xCaO.SiO_2.yH_2O$$
$$+ (3-x)Ca(OH)_2 \tag{1}$$

$$2CaO.SiO_2 + (2+y-x)H_2O \rightarrow xCaO.SiO_2.yH2O$$
$$+ (2-x)Ca(OH)_2 \tag{2}$$

$$3CaO.Al_2O_3 + 3(CaSO_4.2H_2O) + 26H_2O$$
$$\rightarrow 3CaO.Al_2O_3.3CaSO_4.32H_2O \tag{3}$$

$$3CaO.Al_2O_3.3CaSO_4.32H_2O + 2(3CaO.Al_2O_3) + 4H_2O$$
$$\rightarrow 3(4CaO.Al_2O_3.CaSO_4.12H_2O) \tag{4}$$

Both calcium silicates react in a similar way, differing only in the amount of calcium hydroxide, $Ca(OH)_2$, or simply CH, formed (Eqs. 1 and 2). The main reaction product, calcium silicate hydrate ($xCaO.SiO_2.yH_2O$), is called the C-S-H phase. C-S-H is an amorphous phase, in contrast to the crystalline structure of the other hydration product, CH.

C_3A reacts with the added $C\bar{S}H_2$ to form ettringite ($C_6\bar{A}_3H_{32}$), (Eq. 3). When the level of $C\bar{S}H_2$ decreases, the C_3A combines with ettringite to form a monosulfate phase ($C_5A\bar{S}H_{12}$), (Eq. 4).

In the presence of $C\bar{S}H_2$, C_4AF forms the same sequence of hydration products as C_3A, but the reactions are slower. One has to take in to account that all these reactions occur simultaneous in the cement–water system, thus forming a complex but also balanced system. The addition of lignocellulosic materials will undoubtedly affect the hydration process. As referred to in previous publications,[14,15] the lignocellulosic materials seem to have the ability to adsorb cations, particularly calcium, from the cement–water system solution thus affecting the delicate equilibrium of the complex reaction system.

In this work, X-ray diffraction (XRD) and differential thermal analysis (DTA) were used to characterize the cement setting reactions in the absence and presence of selected lignocellulosic materials. XRD detects the crystalline phases present in the starting (nonhydrated) cement, their evolution during hydration, and the new crystalline phases formed as reaction products. In these experiments, only the evolution of CH was monitored, because the main reaction product, C-S-H, is amorphous. In a complementary way, DTA allows the identification of the $C\bar{S}H_2$, CH, and C-S-H phases.

Materials and methods

The lignocellulosic materials used in this study were all of Portuguese origin: cork (the bark of *Quercus suber* L.), pine (*Pinus pinaster* Ait.), and blue gum (*Eucalyptus globulus* Labill.). Blue gum chips were provided by a pulp mill, with a size range of 7–42mm. These were milled further in a Wiley mill to pass through a 6-mm screen. It was assumed that blue gum particles were composed of sapwood, because blue gum trees are usually cut at 10–12 years of age when intended for pulping.

Pine was supplied by a particleboard factory. The particles had a size range of 0.14–5mm, and were taken from the furnish used for the core layer of the panels. Because these particles were sufficiently small, they were not processed further. The pine particles were also assumed to be composed of sapwood. This is because the sources of raw material for the particleboard factory are mainly small round wood, sawmill residues, and slabs from the outer parts of saw logs.

Cork was offered by a cork particleboard factory that uses cork residues from stopper cutting or from low quality cork planks. The fraction applied had a size range of 1–2mm, and it was classified as high density (110–130kg/m³).

Portland cement (CEMI, class 42.5) was used in the mixtures in which 15g of wood or cork (dry basis) were added to 200g of cement. The water added was calculated using the following formula: V (ml of water) = 0.25 (ml/g) × mass of cement (g) + 2.7 (ml/g) × mass of lignocellulosic substrate (g). Four different mixtures were prepared: neat cement; cement, water, and pine (pine mixture); cement, water, and blue gum (blue gum mixture); and cement, water, and cork (cork mixture). The mixtures were transferred to plastic bags, manually moulded in the shape of small boards with dimensions of 200 × 150 × 6mm and left to hydrate at room temperature and humidity. Samples were removed from each mixture after 4, 6, 8, 10, and 12h and then after 1, 1.5, 2, 3, 4, 7, and 28 days of hydration. The samples removed after 4h were obtained with a mortar, but for samples taken after 8h a hammer was required. For those mixtures containing lignocellulosic substrates, a further separation step

was needed to obtain just the cement paste for analysis. For samples less than 12h old, the separation process could be done by manually compressing the samples against a 590-μm sieve, allowing only the cement paste to pass through. Older samples were passed through a 100-μm screen after being separated from the lignocellulosic substrates, and the cement paste was dispersed in 50ml of ethanol and kept in this suspension for 30min to stop the hydration reactions. The material was then filtered and dried at 60°C to constant weight.[16] The dried samples were milled with a mortar to obtain a homogenous powder that was then stored in a desiccator prior to XRD and DTA analysis. In the case of DTA, however, only the samples aged for 4 and 12h, and 2, 7, and 28 days were analyzed.

Results and discussion

X-ray diffraction analysis

The XRD analysis of Portland cement powder allowed the identification of the main phases: C_3S, βC_2S; and the minor phases $C_4(A,F)$, C_3A, and $C\bar{S}H_2$ (Fig. 1). This technique also allowed the monitoring of the hydration cement reactions through the intensity evolution of XRD peaks for each phase. The peaks corresponding to the initial phases present in Portland cement are expected to diminish in intensity and the peaks corresponding to the reaction product, CH, will appear and increase in intensity with time. Due to the amorphous structure of the C-S-H phase, the main reaction product, it cannot be identified by this technique.

Figure 2 presents the XRD results for neat cement after 24h of curing. The $C\bar{S}H_2$ phase was consumed in the initial stages of the hydration reaction, it was barely detected after 4h, and was undetectable after 6h. The product phase CH was detectable after 8h of reaction. The initial material phases, tricalcium silicate and dicalcium silicate, were clearly reduced; as can be deduced from the weakening intensity of their XRD peaks after 4h (Fig. 2) in comparison with the intensity of the same peaks in Fig. 1. The reduction of calcium silicate phases continued during the entire hydra-
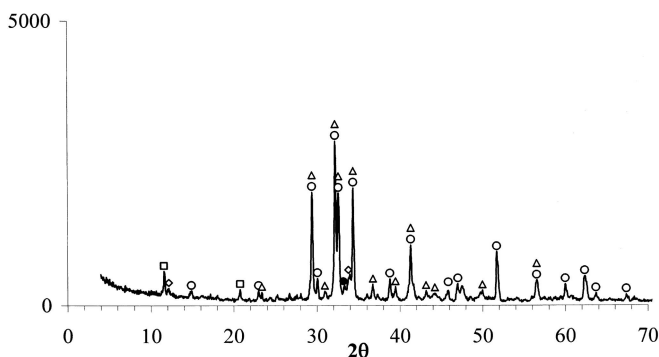
tion period and after 28 days the reaction seemed to be practically complete (Fig. 3). These results for the neat cement can be used to help analyze the hydration behavior of mixtures with lignocellulosic substrates, which generally react more slowly.[17]

Figure 4 shows that some of the $C\bar{S}H_2$ was still present after 12h of reaction when pine particles were present. After 24h, this phase was no longer detected and the first signs of CH appeared. Like neat cement, the intensities of the calcium silicate peaks decreased with time but at a
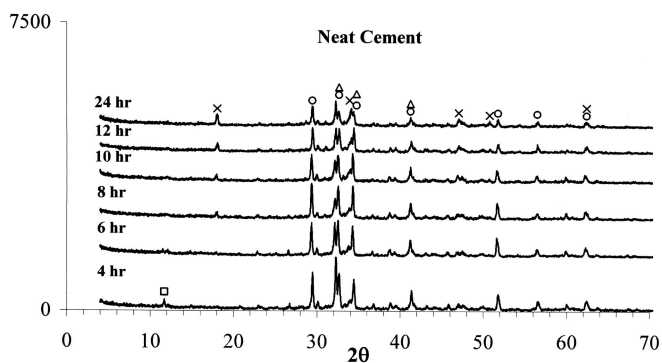
Fig. 2. XRD spectra of hydrated Portland cement (CEMI, class 42.5) for the first 24h of cure. *Circle*, tricalcium silicate; *triangles*, dicalcium silicate; *squares*, calcium sulfate dihydrate; *crosses*, calcium hydroxide
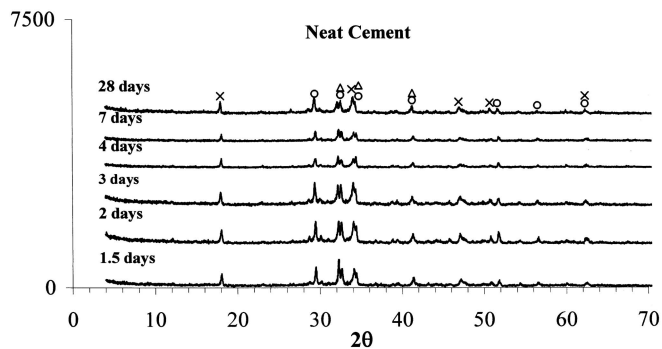
Fig. 3. XRD spectra of hydrated Portland cement (CEMI, class 42.5), between 1.5 days and 28 days of cure. For symbol definitions, see Fig. 2

Fig. 1. X-ray diffraction (XRD) spectrum of nonhydrated Portland cement (CEMI, class 42.5). *Open circles*, tricalcium silicate; *triangles*, dicalcium silicate; *squares*, calcium sulfate dihydrate; *diamonds*, calcium aluminoferrite; *filled circles*, tricalcium aluminate
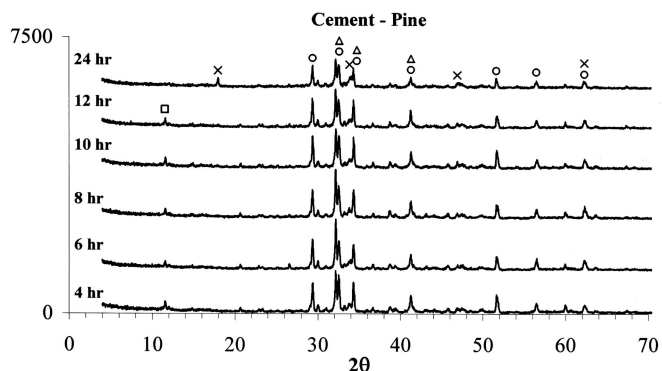
Fig. 4. XRD spectra of hydrated Portland cement (CEMI, class 42.5) for the first 24h of cure in the presence of pine. For symbol definitions, see Fig. 2
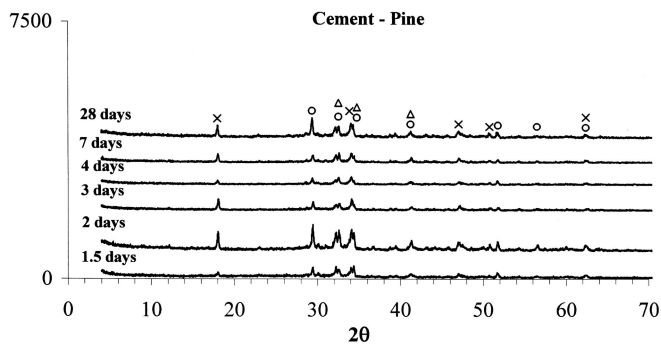
Fig. 5. XRD spectra of hydrated Portland cement (CEMI, class 42.5) between 1.5 days and 28 days of cure in the presence of pine. For symbol definitions, see Fig. 2
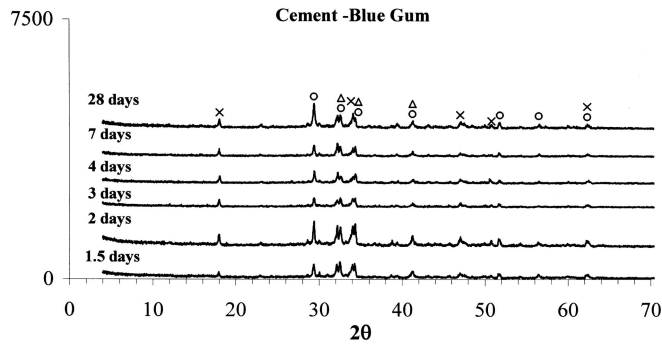

Fig. 7. XRD spectra of hydrated Portland cement (CEMI, class 42.5) between 1.5 days and 28 days of cure in the presence of blue gum. For symbol definitions, see Fig. 2
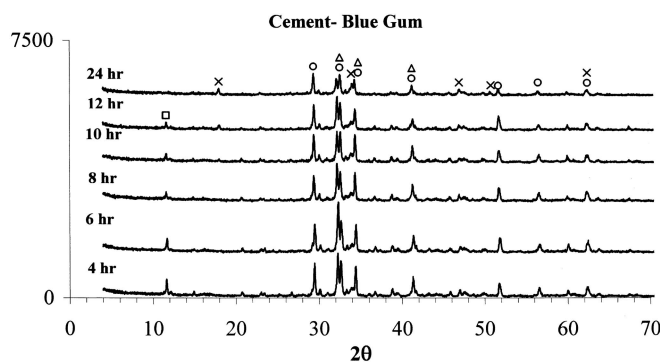

Fig. 6. XRD spectra of hydrated Portland cement (CEMI, class 42.5) for the first 24h of cure in the presence of blue gum. For symbol definitions, see Fig. 2
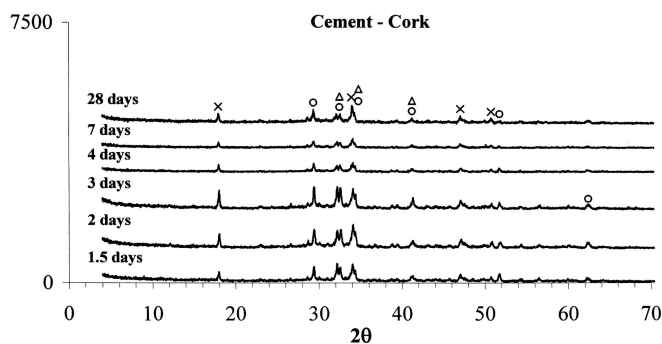

Fig. 8. XRD spectra of hydrated Portland cement (CEMI, class 42.5) between 1.5 days and 28 days of cure in the presence of cork. For symbol definitions, see Fig. 2

slower rate. By comparing Figs. 3 and 5, it can be seen that after 28 days the peaks corresponding to the initial phases of C_3S and βC_2S are not as intense in the neat cement as in the pine mixture. This confirms the slower hydration kinetics of cement when mixed with pine. It was expected that there would be a gradual weakening of the peaks corresponding to the starting C_3S and βC_2S phases with time. However, there is some inconsistency after 24h. For example, the intensity of the relevant peaks seems to be higher after 2 days than after 1.5 days of curing; similarly, the intensity of the peaks after 28 days seems higher than after 3, 4, and 7 days.

Figure 6 shows that the hydration behavior of $C\bar{S}H_2$ in the blue gum mixture was similar to that described for the pine mixture (Fig. 4). In this mixture the presence of CH was detected sooner; after 12h of curing. The hydration behavior of C_3S and βC_2S in the blue gum mixture was also similar to that observed for the pine mixture. The main differences between the pine and blue gum mixtures seem to be in the initial hydration stages, when the reaction kinetics seem to be faster in the case of the blue gum mixture, with $C\bar{S}H_2$ being consumed faster and CH formed sooner. The differences between these two mixtures diminish with hydration time as can be seen by comparing Figs. 5 and 7. This means that, although the starting hydration

kinetics are slower for pine mixtures, the kinetics appear to be enhanced in terms of the hydration time and might even overcome the hydration kinetics for blue gum mixtures.

The unexpected changes in peak intensity described above for the pine mixture after 24h of curing was also observed for the blue gum mixture. In the case of blue gum, however, the characteristic peaks of the C_3S and βC_2S phases were more intense after 2 days than after 1.5 days, and those at 28 days were more intense than at 3, 4, and 7 days.

Among all the lignocellulosic and cement mixtures, the cork mixture achieved the highest degree of hydration, as demonstrated by the low intensity of the peaks for the calcium silicate phases after 28 days (Fig. 8). Nevertheless, in the early stages of hydration (Fig. 9) the reactions seemed to be slower than those of the pine and blue gum mixtures. Even after 4h of hydration, the peaks of the calcium silicates were the most intense of those in the three mixtures. However, this situation was reversed after 8h when the $C\bar{S}H_2$ was hardly detected and completely disappeared after 12h, while the CH began to appear after 12h of hydration, similar to pine, but before blue gum. Once again, the intensity of the characteristic peaks of C_3S and βC_2S phases did not gradually decrease with time. In the specific case of cork
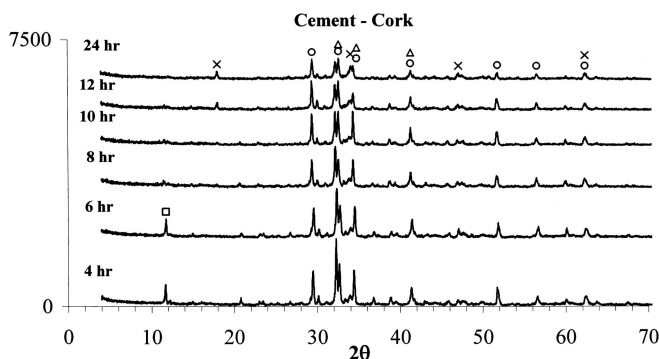
Fig. 9. XRD spectra of hydrated Portland cement (CEMI, class 42.5) for the first 24 h of cure in the presence of cork. For symbol definitions, see Fig. 2

Fig. 10. Differential thermal analysis (DTA) curves of nonhydrated and hydrated Portland cement (CEMI, class 42.5) for up to 28 days of cure

Fig. 11. DTA curves of nonhydrated and hydrated Portland cement (CEMI, class 42.5) for up to 28 days of cure in the presence of pine

mixture, the peaks after 4 and 7 days were less intense than those after 28 days of curing.

The irregular behavior in intensity of peaks for the C_3S and βC_2S phases was also observed for neat cement. In summary, the trend seems to be for an increasing intensity of peaks corresponding to the starting phases and of the reaction product CH, within the hydration time period between 7 and 28 days. Within the hydration time period between 3 and 7 days there was an apparent decreasing intensity of peaks corresponding to the CH phase.

Differential thermal analysis

Differential thermal analysis allows the detection of the principal reaction product, the C-S-H phase, therefore giving complementary information to that obtained from the XRD technique. For a nonhydrated Portland cement, the two characteristic DTA peaks between room temperature and 600°C are endothermic due to thermal decomposition of $C\bar{S}H_2$ within the temperature range of 145°–165°C, and CH at 485°C, which is possibly formed during storage as a result of contact with water vapor present in the atmosphere.[18] According to Taylor,[18] the C-S-H phase is thought to occur between 115° and 125°C and the characteristic endothermic peak of CH shifts to between 530° and 550°C because the extended degrees of hydration cause larger crystals. All these reference values are theoretical, and in practice they can deviate.

The DTA curve for nonhydrated cement is shown in Figs. 10 to 13 for comparison with the other curves. It shows the peaks corresponding to $C\bar{S}H_2$ and CH formed during storage are centred at 141°C and 448°C, respectively. As the curing time increases, the CH peaks tend to appear at higher temperatures, which is consistent with the formation of larger CH crystals developed in the presence of liquid water during the normal cement hydration process. For the neat cement mixture (Fig. 10), the $C\bar{S}H_2$ detected after 4 h of curing was consumed after 12 h. CH was first detected after 12 h and was always subsequently present. Although the shorter hydration time intervals between XRD analyzes enabled a more accurate determination of the curing times at which the $C\bar{S}H_2$ and CH phases were consumed and
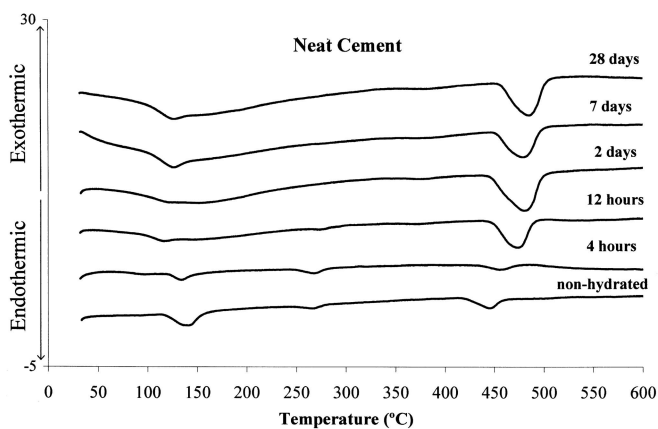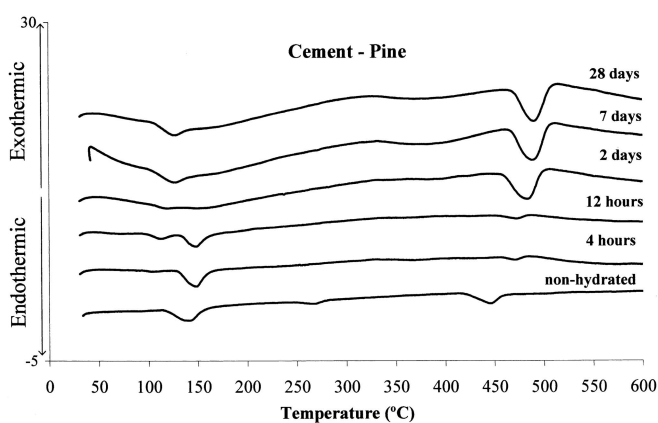
formed, respectively, the DTA results presented in Fig. 10 seem to be in good agreement with the XRD data. DTA identified the C-S-H phase after 7 days of curing with its characteristic decomposition peak at 129°C. Even though the ettringite could produce a characteristic peak at 135°–140°C,[18] its presence is unlikely because this phase cannot be detected by XRD, and, if formed, this phase would reach its maximum concentration between 16 and 24 h.[18]

For the pine mixture, the $C\bar{S}H_2$ phase was present for at least 12 h of curing (peak at 150°C, Fig. 11), and was consumed by the end of 2 days. The first sign of C-S-H presence is visible in Fig. 11 after 12 h of hydration. Although its presence was not apparent in the 2-day-old sample, it reappears, and is significant, in the 7-day-old sample. CH was detected by DTA after 2 days of curing (peak at 487°C, Fig. 11). It is possible that it could have formed sooner, between 12 and 24 h, because the XRD analyzes shown in Fig. 4 indicate that it formed by the end of 24 h of hydration. From these results one can conclude that, as expected, the hydration kinetics for the pine mixture are slower than for the neat cement. Accordingly, the $C\bar{S}H_2$ phase took longer to be consumed and the CH only appeared after longer hydration times.
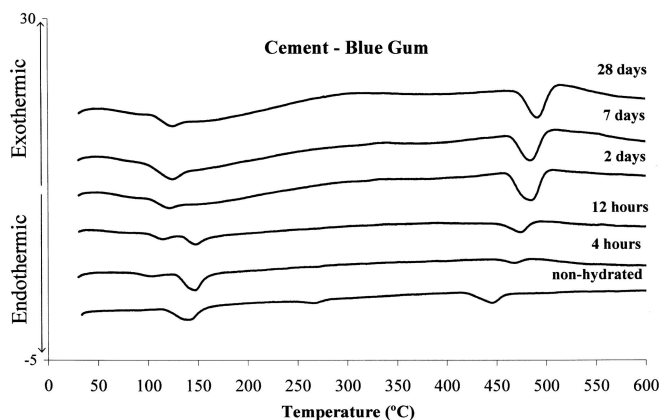
Fig. 12. DTA curves of nonhydrated and hydrated Portland cement (CEMI, class 42.5) for up to 28 days of cure in the presence of blue gum
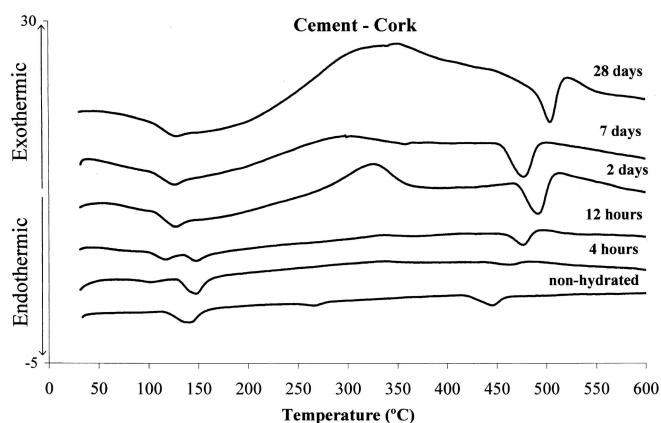

Fig. 13. DTA curves of nonhydrated and hydrated Portland cement (CEMI, class 42.5) for up to 28 days of cure in the presence of cork

The behavior of the blue gum mixture was similar to that of the pine mixture. The $C\bar{S}H_2$ was present for at least 12 h, which is the same time that the C-S-H phase appears (peak at 115°C, Fig. 12). Figure 12 also shows that for longer curing times, the characteristic peak of the C-S-H phase also appears but is slightly dislocated to higher temperatures: 124°C, 127°C, and 128°C for 2, 7, and 28 days, respectively. DTA detected the CH at the end of 4 h of curing (peak at 470°C, Fig. 12), which was sooner than with XRD. Nevertheless, its presence was more significant after 12 h of curing, which is shown by a more intense peak at 477°C for the 12-h curve in Fig. 12. Again the DTA results are in good agreement with the XRD results, reinforcing the conclusion that the main differences in the hydration kinetics between the pine and blue gum mixtures seem to occur in the earlier stages of reaction, where the blue gum mixture exhibits faster kinetics.

Figure 13 shows the DTA results for the cork mixtures. The curves reveal a new feature, namely, large exothermic peaks between 310° and 370°C for curing times greater than 2 days. These peaks are not due to any transformation within the cement but are due to the presence and conse-

quent burning of organic material that could not be removed from samples. The exothermic peaks are present in the older samples because it became increasingly difficult to remove the cork as the cement hardened.

Figure 13 also shows that the $C\bar{S}H_2$ in the cork mixture was not entirely consumed until after 12 h of curing or more, because its characteristic peak at 150°C is still present. With this phase being barely detected by XRD after 8 h of curing and not at all after 12 h, these results suggest that DTA might be more sensitive to the presence of small amounts of $C\bar{S}H_2$ than XRD. The peak centred at 480°C in the 12-h curve in Fig. 13 can be assigned the initial formation of CH. A peak centred at 120°C, corresponding to the C-S-H phase, is just visible after 4 h of curing and intensifies with time.

The XRD and DTA results presented here are consistent with the temperature profiles and compatibility indexes presented previously.[17] In fact, the mixtures with cork presented, in general, the best compatibility indexes, indicating that it has the least effect on the hydration reactions.[17] Conversely, the compatibility indexes determined for pine were the worst, showing that pine has a more negative effect on cement hydration during the first 24 h, and the results obtained in this present work confirm this.

Conclusions

As expected, all three lignocellulosic substrates used in this work had a detrimental effect on cement hydration. The pine and blue gum mixtures presented similar behaviors, differing only in the initial stages of reaction when the blue gum permits faster hydration kinetics. However, the extents of the reactions at the end of the hydration period were very similar for both mixtures as demonstrated by the similar peak intensities of the calcium silicate phases after 28 days of curing.

In the early stages of curing, cork seemed to be the inhibitory substrate. This could be expected considering its higher extractive contents when compared with the other two substrates.[15] Nevertheless, as curing time increases it becomes clear that cork is the most compatible of the three substrates. It is possible that the other two substrates might adsorb more cations from the cement–water solution, thus affecting, in another way, the delicate equilibrium of the complex reaction system.[14,15]

The XRD and DTA techniques used in this work provide useful data for the comprehension of phenomena occurring during the setting of cement in the presence of lignocellulosic substrates. They allow the determination of when certain phases such as CH, C-S-H, and $C\bar{S}H_2$ appear or are consumed. Moreover, both techniques confirmed the conclusions drawn from temperature profile measurements made previously.[17]

Madeiras e Derivados, and Secil – Companhia Geral de Cal e Cimento for providing cork granules, eucalypt chips, pine particles, and the cement, respectively.

References

1. Wei YM, Zhou YG, Tomita B (2000) Hydration behavior of wood cement-based composite I: evaluation of wood species effects on compatibility and strength with ordinary Portland cement. J Wood Sci 46:296–302
2. Miller DP, Moslemi AA (1991) Wood–cement composites: species and heartwood-sapwood effects on hydration and tensile strength. Forest Prod J 41:9–14
3. Miller DP, Moslemi AA (1991) Wood–cement composites: effect of model compounds on hydration characteristics and tensile strength. Wood Fiber Sci 23:472–482
4. Semple KE, Cunningham RB, Evans PD (1999) Cement hydration tests using wood flour may not predict the suitability of *Acacia mangium* and *Eucalyptus pellita* for the manufacture of wood-wool cement boards. Holzforschung 53:327–332
5. Alberto MM, Mougel E, Zoulalian A (2000) Compatibility of some tropical hardwoods species with Portland cement using isothermal calorimetry. Forest Prod J 50:83–88
6. Wolfe RW, Gjinolli A (1999) Durability and strength of cement-bonded wood particle composites made from construction waste. Forest Prod J 49:24–31
7. Schmidt R, Marsh R, Balatinecz JJ, Cooper PA (1994) Increased wood–cement compatibility of chromated-treated wood. Forest Prod J 44:44–46
8. Ramirez-Coretti A, Eckelman CA, Wolfe RW (1998) Inorganic-bonded composite wood panel systems for low-cost housing: a Central American perspective. Forest Prod J 48:62–68
9. Rashwan MS, Hatzinikolas M, Zmavc R (1992) Development of a lightweight, low-cost concrete block using wood residue. Forest Prod J 42:57–64
10. Hachmi M, Moslemi AA (1989) Correlation between wood–cement compatibility and wood extractives. Forest Prod J 39:55–58
11. Hachmi M, Moslemi AA (1990) Effect of wood pH and buffering capacity on wood–cement compatibility. Holzforschung 44:425–430
12. Jackson PJ (1998) Portland cement: classification and manufacture. In: Hewlett PC (ed) Lea's chemistry of cement and concrete, 4 edn. Butterworth-Hinemann, Oxford
13. Odler I (1998) Hydration, setting and hardening of portland cement. In: Hewlett PC (ed) Lea's chemistry of cement and concrete, 4 edn. Butterworth-Hinemann, Oxford
14. Pereira C, Caldeira Jorge F, Irle MA, Ferreira JM (2002) The interaction of calcium and other cations with lignocellulosic substrates, and their influence on cement setting. Proceedings of the 6th European Panel Products Symposium, Llandudno, North Wales, UK, 9–11 October 2002
15. Pereira C, Caldeira Jorge F, Irle MA, Ferreira JM (2003) Extractive contents of two woods and cork of Portuguese origin and the interaction of these substrates with cement suspensions. Forest Prod J 53:39–43
16. Fumo DA (1997) Cements in refractory LCC and ULCC concretes: synthesis, hydration mechanism and interaction with microfillers (in Portuguese). PhD Thesis, University of Aveiro
17. Pereira C, Caldeira Jorge F, Irle M, Ferreira JM (2006) Characterizing the setting of cement when mixed with cork, blue gum, or maritime pine, grown in Portugal I: temperature profiles and compatibility indices. J Wood Sci DOI 10.1007/S10086-005-0774-z
18. Taylor HFW (1997) Hydration of Portland cement. In: Cement chemistry, 2nd edn. Thomas Telford, London